Published in final edited form as:
Cancer Invest. 2009 March ; 27(3): 264–272. doi:10.1080/07357900802406319.

PDLIM4, An Actin Binding Protein, Suppresses Prostate Cancer Cell Growth

Donkena Krishna Vanaja, **Michael E. Grossmann**, **John C. Cheville**, **Mozammel H. Gazi**, **Aiyu Gong**, **Jin San Zhang**, **Katalin Ajtai**, **Thomas P. Burghardt**, and **Charles Y. F. Young**
Departments of Urology and Biochemistry and Molecular Biology, Mayo Clinic College of Medicine, Mayo Clinic, Rochester, MN, USA

Abstract

We investigated the molecular function of PDLIM4 in prostate cancer cells. PDLIM4 mRNA and protein-expression levels were reduced in LNCaP, LAPC4, DU145, CWR22, and PC3 prostate cancer cells. The re-expression of PDLIM4 in prostate cancer cells has significantly reduced the cell growth and clonogenicity with G1 phase of cell-cycle arrest. We have shown the direct interaction of PDLIM4 with F-actin. Restoration of PDLIM4 expression resulted in reduction of tumor growth in xenografts. These results suggest that PDLIM4 may function as a tumor suppressor, involved in the control of cell proliferation by associating with actin in prostate cancer cells.

Keywords

Prostate cancer; Tumor suppressor gene; LIM domain protein; Cell growth; Actin cytoskeleton

INTRODUCTION

Multiple molecular alterations occur during cancer development (1). A number of laboratories have implemented DNA microarrays to analyze genes deregulated in prostate cancer (2–6). In our previous gene-profiling studies with a cohort of prostate cancer tissues we have reported underexpression of PDLIM4 in cancer tissues by hypermethylation (5). In fact, as determined by the real-time reverse transcriptase-polymerase chain reaction (RT-PCR) analysis, an average of 2.8-, 4.0- and 10.6-fold decrease in PDLIM4 transcript level was observed in intermediate grade (Gleason score 6), high-grade (Gleason score 9), and metastatic tumors, respectively, when compared with benign epithelia (5). In support of our observation, several microarray expression profiles have shown downregulation of PDLIM4 in prostate cancer tissues (5, 7, 8). Inactivation of PDLIM4 is also observed in acute myelogenous leukemia and colon cancer by hypermethylation (9). The frequent transcriptional silencing in several tumor tissues (10, 11) indicates that PDLIM4 may play a role as tumor suppressor and could be involved in prostate cancer development or progression.

PDZ/LIM genes encode a group of proteins that play very important, but diverse, biological roles (12). Several recently identified PDZ-LIM proteins have been suggested to participate in many fundamental biological processes such as cytoskeleton organization, neuronal

Correspondence to: Charles Y. F. Young, Ph.D., Professor, Department of Urology and Biochemistry and Molecular Biology, Guggenheim 520 C, Mayo Clinic College of Medicine, 200 1st street S.W., Rochester, MN 55905, USA, youngc@mayo.edu.
Dr. Vanaja DK and Dr. Grossman ME contributed equally to this study.

signaling, cell-lineage specification, and organ development as well as pathological processes like oncogenesis (13). Ten genes have been reported that encode for a PDZ domain and one or several LIM domains: four genes of the ALP subfamily (ALP, Elfin, Mystique, and PDLIM4), three of the Enigma subfamily (Enigma, Enigma Homolog, and ZASP), the two LIM kinases (LIMK1 and LIMK2), and the LIM only protein 7 (LMO7) (14). Functionally, all PDZ and LIM-domain proteins share an important trait, i.e., they can associate with and/or influence the actin cytoskeleton (15). PDZ-LIM proteins act as adapters recruiting signaling molecules to the actin cytoskeleton (16). They associate with the actin cytoskeleton via their PDZ domains (17), and with kinases via their LIM domains (18). The LIM-domain proteins have been found to be expressed in prostatic epithelial cells as well as cancerous cells including ARA55/Hic5, FHL2, PCD1, TES, and PINCH (19–23). LIM-domain genes that have been proposed to be tumor suppressors include TES (24), LIMD1 (25), Limatin (26), and EPLIN (27). Both TES and EPLIN were shown to be associated with actin and capable of suppressing cell motility or anchorage independent growth of transformed cells. The PDLIM4 LIM domain can interact with PDZ domains in the protein tyrosine phosphatase PTP-BL, and with the PDZ domain of PDLIM4 itself (28). In addition, the PDZ domain of PDLIM4 was shown to interact with the second LIM domain, TRIP6, a protein containing three C-terminal LIM domains (29). However, there is no clear evidence showing the role of PDLIM4 gene in prostate cancer. To investigate the molecular function of PDLIM4, we first analyzed the expression of PDLIM4 in several prostate cancer cell lines. We have shown the down regulation of mRNA and protein expression levels in DU145, LAPC4, LNCaP, CWR22 and PC3 prostate cancer cells. Further, Immunohistochemistry analysis indicated that PDLIM4 protein expression was highly restricted to the secretory epithelial cells in human prostate tissues and markedly reduced expression was observed in prostatic adenocarcinoma. We cloned the PDLIM4 cDNA from normal human prostate cell line RWPE1 and expressed the full length protein in the prostate cancer cell lines. The reexpression has lead to a suppression of cell growth and colony formation in soft agar. Our assays revealed direct interaction of PDLIM4 protein and F-actin. Finally, transfection of the prostate cancer cells with PDLIM4 expression vector suppressed the tumor development in xenografts.

MATERIAL AND METHODS

Cell culture and Western blot

Prostate cancer cells DU145, LAPC4, LNCaP, CWR22, and PC3 were grown in RPMI 1640 medium (Life Technologies, Baltimore MD), with 2 mM L-glutamine (Life Technologies, Baltimore MD), 5% fetal calf serum (FCS) (HyClone, Logan, UT), 25 units/mL penicillin and 25 μg/mL streptomycin (Life Technologies, Baltimore MD). The nontumorigenic RWPE-1 cells (21) were grown in complete keratinocyte-SFM medium (Invitrogen, Grand Island, NY). After 42 hr of culture, cells (1×10^6 cells) were sonicated and equal aliquots of whole cell lysates were run on a 4–12% gradient NuPAGE gel in 1× MES SDS running buffer (Invitrogen). The separated proteins were transferred onto nitrocellulose membrane, blotted with an anti-PDLIM4 antibody or anti-V5 antibody (Novus Biologicals, Littleton, CO) and visualized using SuperSignal™ West Dura (Pierce, Rockford, IL) according to manufacturer's instructions.

Isolation of RNA and semi-quantitative PCR

Total RNA was isolated from prostate cancer cell lines as described previously (4). In brief, total RNA was extracted using TRIzol reagent (Life Technologies, Inc., Carlsbad, CA). DNA contamination was removed using DNA-free kit (Ambion, Austin, TX), and RNA cleanup was performed using RNeasy Mini kit (Qiagen, Valencia, CA). First-strand cDNA synthesis was done by 1 μg of total RNA. Semiquantitative PCR was performed for analysis

for PDLIM4 expression. A forward primer 5′ ACT TCA GCG CGC CCC TCA CCA TCT CAC 3′ and a reverse primer 5′ TCT AGC ATG CCC TGC AAG TAG CGG AAG G 3′ was used in the PCR for PDLIM4 expression. GAPDH expression levels were used as normalization controls (30).

Generation of DNA constructs and protein purification

A pair of primers (a forward primer, 5′ CAG GCC GCC ATG CCC CAT TCC GTG A 3′ and a reverse primer, 5′ GAC GAG TTC CAC CTT GGC ATT GG 3′) encompassing the entire PDLIM4 open-reading frame (GenBank number BC016765) were used to perform PCR on cDNA generated from RWPE-1 cells. The resulting products were then subcloned into the pcDNA3.1/V5-His TOPO TA mammalian-expression vector (Invitrogen) or pGEX-5X-1 Glutathione S transferase (GST) bacterial-expression vector (Amersham Pharmacia Biotech, Piscataway, NJ). The identity of the inserted cDNA sequences were confirmed by sequencing. GST-PDLIM4 and GST protein produced from pGEX-5X-1-PDLIM4 and pGEX-5X-1-GST vectors in bacteria, respectively, were purified using the Bulk GST Purification Module (Amersham Biosciences, Piscataway) as per the manufacturer's instructions, with the purified protein being released by addition of glutathione elution buffer. GST-PDLIM4 protein was also used to produce an anti-PDLIM4 rabbit polyclonal antibody. The antiserum was affinity purified with GST-PDLIM4 and Aminolink plus Coupling Gel (Pierce, Rochford, IL).

Immunohistochemistry staining

Surgically resected prostate tissue specimens were obtained from patients who had undergone radical prostatectomy at Mayo Clinic with Institutional Review Board approval. All tissues were collected from the Mayo Clinic Tissue Registry and the prostate SPORE Tissue Core. Sections of 4-μm size were cut from neutral buffered formalin-fixed, paraffin-embedded tissue blocks from four intermediate-grade (primary stage T2 Gleason score 6 of pattern 3 + 3) and four high-grade (primary stage T3 Gleason score 9 of pattern 4 + 5) prostatic adenocarcinoma patients along with four separately collected nonmalignant benign prostatic tissue samples. All slides were reviewed by a pathologist (J.C.C.) for appropriate identification of the Gleason pattern and benign acini. No patients had received preoperative therapy such as radiation or androgen deprivation. Standard biotin–avidin complex immunohistochemistry was used for evaluation of the PDLIM4 expression. Affinity-purified rabbit anti-PDLIM4 antibody was used at a dilution of 1:1000. The secondary anti-rabbit PDLIM4 antibody was applied for 30 min, and the enzyme reaction was completed with the use of a streptavidin biotin detection kit (DAKO Deceloping System, Carpinteria, CA). The slides were developed with diaminobenzidine for 5 min. Digital images were captured on an Axioplan 2 upright microscope equipped with KS400 image-analysis software (Carl Zeiss, Inc., Oberkochen, Germany).

Cell growth and cell-cycle analyses

To determine the effect of PDLIM4 on cell growth, PDLIM4-V5 expression vector (pcDNA3.1/V5-His TOPO TA vector) or empty vector was transfected into the DU145 and LNCaP prostate cancer cell lines. An enhanced green fluorescent protein (EGFP) expression vector with the above vectors was also cotransfected to these cell lines. After 48 hr of transfection, both cells were trypsinized and single cells with GFP fluorescence were sorted by a cell-sorting device. FACS (FACS Vintage Cell Sorter) was employed to enrich cells expressing green fluorescence after being cotransfected with PDLIM4 and enhanced green fluorescent protein (EGFP) for cell-proliferation assay. Equal numbers of sorted cells were placed into 96-well plates with a 5% FCS growth medium. PC3 cells were also transfected with the above PDLIM4 expression vector or with the empty vector and after 24 hr selection medium containing 400–600 μg/mL G418 (Life Technologies, Baltimore, MD) was added.

Individual stably transfected PC3 clones were then isolated and grown in the selection medium. Western blot analysis was performed to test for the presence of the PDLIM4 V5 expression using the V5 antibody in the whole-cell extracts. To assess the cell growth, 1×10^3 cells with PDLIM4 expression vector or empty vectors clones 1 and 2 were plated in triplicate in a 96-well plate and MTS assay (3-(4, 5-dimethylthiazol-2-yl)-5-(3-carboxy-methoxyphenyl)-2-(4-sulfophenyl)-2H-tetrazolium) (Promega, Madison, WI) was used to measure cell growth on day 1, 4, and 7. Cell growth of RWPE-1 cells expressing endogenous PDLIM4 was also measured over 7 days.

For cell-cycle analysis, after 48 hr of serum-free starvation, PDLIM4 or control vector stably transfected PC3 cells were split by trypsin and seeded at 6.25×10^5 per 10-cm dish. After 20 hr, cells were trypsinized, washed twice with PBS, and fixed in ice-cold 40% ethanol. Fixed cells were incubated with 10 μg/mL RNase (Roche Diagnostics Corporation, Indianapolis, IN) at 37°C for 15 min, stained with 10 μg/mL propidium iodide (Sigma) at room temperature, and analyzed on a FACScan flow cytometer. The percentage of cells in different phases of the cell cycle was determined using ModFit cell-cycle-analysis software.

Soft agar colony formation assay

To evaluate the role of PDLIM4 in malignant transformation of cells, we performed anchorage independent growth assay in soft agar. Prostate cancer cell lines PC-3 and DU145 were plated and transfected with PDLIM4-V5 expression vector or control empty vector as described above. After 24 hr of transfection the cells were trypsinized, counted, and plated on soft agar at 1×10^5 cells per well in six-well plates. Prior to cell plating, 1.0 mL of 0.6% Noble agar (Becton Dickinson and Company, Franklin Lakes, NJ) in the RPMI 1640 medium containing 400 μg/mL of G418 was allowed to solidify in each well. The transfected cells were then mixed to a final volume of 2.0 mL per well in 0.3% Noble agar in RPMI 1640 media with G418 and layered over the 0.6% layer of Noble agar. Transfection efficiency was justified by equal number of cells expressing fluorescent EGFP. One milliliter of 0.3% agar in RPMI 1640 media with G418 was overlaid each week. The cells were stained with 0.1% crystal violet (Sigma) and the colonies greater than 200 μm were counted after four weeks.

F-actin-binding assay for localization of PDLIM4

Although PDLIM4 was identified as a cytoskeleton associated protein and can bind several proteins like actinin (23) and TRIP6 (24), but the mechanism of action in prostate cancer is not clear. To study the association of PDLIM4 with actin cytoskeleton, F-actin cosedimentation assay was performed as described previously (20, 21) using the Actin Binding Protein Biochem Kit (Cytoskeleton Inc. Denver, CO) and the recombinant GST-PDLIM4. Various concentrations of GST-PDLIM4 (0, 4.0, 6.0, and 8.0 μg) were mixed with 50 μg of F-actin in 50 μL of buffer (10 mM Tris HCl pH 7.5, 0.2 mM $CaCl_2$, 0.5 mM DTT, 0.1 mM PMSF, 1.0 mM $MgCl_2$, 60 mM KCl) at 24°C for 20 min and centrifuged at 100,000 g at 24°C for 20 min. GST-PDLIM4 (8.0 μg) without actin was used as control for the cosedimentation assay. The supernatants were then removed and the cell pellets resuspended in the same buffer. Aliquots of cell pellet and supernatants were mixed with the loading dye and the fractions were then run on a 4–12% gradient NuPAGE gel in 1× MES SDS running buffer for Western blot analysis using an anti-GST antibody (Amersham Biosciences, NJ).

Detection of PDLIM4 in cells by immunofluorescence

We performed immunofluorescence in prostate cancer cells to determine the localization and the distribution of PDLIM4 in prostate cancer cells. Three human prostate cell lines, RWPE-1, PC-3, and DU145, were grown on glass slides precoated with fibronectin (Sigma, Saint Louis, MO). For transfection, cells were plated in culture dishes or on 10-well HTC

super-cured glass slides (Cel-line/Erie Scientific Co. Portmouth, NH) and grown to 50–80% confluence and transfected with Lipofectamine (Invitrogen) as per manufacturer's direction. PC-3 and DU145 cells were transfected with PDLIM4-V5 expression vector (pcDNA3.1/V5-His TOPO TA vector) or a control empty vector for 24 hr. Cells were fixed with 4% paraformaldehyde, permeabilized with Triton × 100, incubated with anti-V5 antibody (Novus Biologicals Inc. Littleton, CO), anti-PDLIM4 antibody, and then stained with FITC-conjugated second antibody, goat anti-rabbit IgG, (Molecular Probes Inc. Eugene, OR) for PDLIM4-V5 or PDLIM4 (green) and rhodamine-conjugated phalloidin (Molecular Probes Inc) for F-actin (red). Fluorescent images were captured in a Zeiss LSM 510 laser-scanning confocal microscope (Carl Zeiss Microimaging Inc. Thornwood, NY).

In vivo growth assay

To determine the effect of PDLIM4 on *in vivo* tumor growth, stably transfected PC3 cells (1×10^6 cells/mouse) expressing PDLIM4-V5 expression vector or empty vector (internal control) mentioned above were injected subcutaneously into both flanks in the hinder region of athymic BALB/c mice in 0.1 ml of phosphate buffered saline as approved by Mayo Clinic Institutional Animal Care and Use Committee. Four mice were used in each group. Tumor growth was measured twice weekly to check for the palpable tumors. From the time of palpable tumors, tumor growth was recorded every week up to 8 weeks. Tumor volume was calculated as length × height × width × 0.5236 (22). Tumor sizes were reported as mean volumes ± standard deviation (SD).

Statistical analysis

All cell-growth and colony-formation assays on cells were done three separate times, and the values are given as mean ± SD. Mean of groups for cell growth, colony formation, and *in vivo* tumor-growth assays were compared with the Student's *t* test and *p*-value <0.05 was accepted as the level of significance.

RESULTS

Expression of PDLIM4 in prostate cancer cell lines and tissues

Transcription levels of PDLIM4 in human prostate cancer cell lines determined by RT-PCR revealed that the expression is undetectable in tumor-forming cell lines DU145, CWR22, LNCaP, and LAPC4 cells compared to the nontumor-forming cell line RWPE-1, suggesting its potential biological relevance to prostate cancer. Intriguingly, PDLIM4 mRNA is expressed in PC3 cell lines but the expression is roughly about half of that found in the nontumorigenic RWPE1 cells (Figure 1A). Moreover, Western blot analysis of PDLIM4 protein in these cell lines (Figure 1B) correlated well with the PDLIM4 mRNA levels. To study PDLIM4 expression further in human tissues and to explore its potential as a molecular marker, we performed immunohistochemistry staining of a panel of human tissues by using anti-PDLIM4 antibody. PDLIM4 immunoreactivity was restricted to the subpopulation of secretory epithelial cells in the benign tissues and a reduced level of staining was seen in the prostate cancer tissues (Figure 1C).

PDLIM4 suppresses in vitro growth of prostate cancer cells

To investigate whether PDLIM4 expression can affect prostate cancer cell growth, we transfected the PDLIM4 cDNA (described in materials and methods) into the prostate cancer cell lines LNCaP, DU145, and PC3. The results indicated that cell-growth rates were significantly reduced ($p < 0.05$) by expression of PDLIM4 in LNCaP and DU145 cell lines (Figure 2A). Western blot analysis of PDLIM4-transfected stable cells revealed that the exogenous PDLIM4 is about 80% of endogenous PDLIM4 by densitometry. The size of

exogenous PDLIM4 is larger than endogenous PDLIM4 due to the V5 tag. The PDLIM4-stable PC-3 clone exhibits significant growth inhibition on day 7 compared with the vector clones of PC3 cells with endogenous PDLIM4 and nontumorigenic RWPE-1 cells with endogenous PDLIM4 (Figure 2B). Taken together, these results demonstrate that ectopically re-expressed PDLIM4 can suppress cell growth in human prostate cancer cell lines tested.

Furthermore, soft agar assay was used to test whether PDLIM4 can reduce colony formation of PC-3 and DU145 cells in soft agar. There were fewer colonies formed from the PDLIM4-transfected PC3 and DU145 cells compared (35% and 39%, respectively vs. 100% control) with control vector-transfected cells (Figure 2C). These results were statistically significant with a $p < 0.001$. In order to understand the mechanism of PDLIM4 growth inhibition, we performed FACScan flow cytometry analysis of the PC3 cells stably transfected with PDLIM4 or vector to determine the percentage of cells in G1, G2, or S phase. The cells ectopically expressing PDLIM4 had 62.59% of the cells in G1 while the vector control cells had only 40.30% of the cells in G1 (Figure 2D). There was no significant apoptotic DNA observed. These suggest that PDLIM4 may play a role in preventing the cells moving into the DNA synthesis S phase from the arrest of cytoplasmic active G1 phase.

PDLIM4 association with F-actin

We used purified recombinant GST-PDLIM4 in an *in vitro* cosedimentation assay to investigate the interaction of PDLIM4 and F-actin. The polymerized actin (F-actin), which is formed from G-actin, was incubated with GST-PDLIM4 or GST fraction alone. The samples were subjected to SDS-PAGE separation after fractionation. Actin was detected in the cell pellet fractions of both GST-PDLIM4 and GST, whereas the GST-PDLIM4 but not GST could be brought down significantly to sediments by F-actin (Figure 3A). With increasing concentration of GST-PDLIM4, we observed increased amounts of PDLIM4 in the pellet (Figure 3B). Immunofluorescence/confocal microscopy were performed to further confirm the association of PDLIM4 protein with actin. Endogenous PDLIM4 was found to be colocalized with F-actin in stress fibers in the nontransfected RWPE-1 cells. Indeed, the ectopically expressed PDLIM4 visualized by anti-V5 antibody was found to be colocalized with F-actin in stress fibers as well as ruffles in DU145 and PC3 cells (Figure 4). These results suggest for the first time that PDLIM4 could directly interact with F-actin.

Tumor inhibitory potential of PDLIM4

To assess the effect of PDLIM4 on tumor growth, *in vivo* growth assay was performed in athymic mice with the PDLIM4 stably transfectanted PC3 cells and an empty vector-transfected PC3 cells. The result of this preliminary xenograft study showed that none of the mice inoculated with PDLIM4 stable cells exhibited any significant signs of tumor growth, whereas the empty vector stable cells produced significant tumor mass in various sizes at 6, 7, and 8 weeks of post-inoculation ($p < 0.05$), indicating that PDLIM4 can cause inhibition of PC-3 tumor growth *in vivo* (Figure 5). Because the number of animals used in this preliminary study is limited, these findings need further validation in large study group to confirm the inhibition potential of PDLIM4 on tumor growth.

DISCUSSION

We have previously reported that PDLIM4 is silenced in prostate cancer (5), but the biological function and disease relevance has not been examined. In this study, we showed the PDLIM4 expression is downregulated or lost in human prostate cancer cell lines both at mRNA and protein levels. The loss of expression in high-grade prostate cancer tissues and in cell lines DU145, LAPC4, LNCaP, and CWR22 may be due to complete promoter hypermethylation of both the alleles, whereas the underexpression of PDLIM4 in PC-3 cells

may reflect partial methylation of its promoter. Our data is consistent with a recent report that showed that PDLIM4 expression is lost in other cancer cell lines (Raji, Dupro, HCT116, RKO, and SW48), whereas cell lines with low (U373) or partial methylation (K562) retained expression (9). PDLIM4 maps to 5q31.1 (31), a locus involved in neoplastic transformation in acute myelogenous leukemia and which has been suspected to harbor a tumor suppressor gene for many years (32). PDLIM4 is thus far the only gene described in the 5q31 region that is frequently inactivated biallelically due to a combination of LOH and methylation (31). Further genetic and epigenetic studies are required to address the effect of LOH and methylation on the transcriptional silencing of PDLIM4 in prostate cancer cells.

Re-expression of cytoskeletal-associated genes in cell lines was reported to inactivate some important features of transformation such as restoration of focal adhesion and cytoskeletal structures, cell contact growth inhibition, inability of anchorage-independent growth, and cellular tumorigenicity. We tested with three prostate cancer cell lines to demonstrate that indeed the re-expression of PDLIM4 exhibits growth-inhibitory effect. PDLIM4 overexpression inhibited both anchorage-dependent and -independent growth in LNCaP, DU145, and PC3 prostate cancer cells. Intriguingly, the parental PC-3 cells express some endogenous PDLIM4 but the amounts are lower than that in nontumorigenic RWPE-1 cells. However, all cells tested with ectopically expressed PDLIM4 seem to exhibit similar growth-inhibition effects. This may indicate that parental PC-3 has adapted to the relatively low level of PDLIM4 to establish its growth rate. A moderate increase in PDLIM4 ectopically to the range of normal levels (in reference to that in RWPE-1 cells in Figures 1A and 1B) might be enough to make cells sensitive to growth regulation by PDLIM4. The suppression of colony formation in the soft agar assay by overexpression of PDLIM4 in PC3 and DU145 cells suggests that PDLIM4 may play a role in inhibition of tumor cell invasion. The dramatic decrease (<10.6 fold) in the mRNA expression of PDLIM4 in metastatic tumors supports this hypothesis (5). The cell-cycle arrest in G1 phase by overexpression suggests that PDLIM4 may play a role in controlling inhibition of cell proliferation by protein–protein interaction in the cytoplasm preventing the cells to enter the S phase. Taken together, the suppression of cell growth and inhibition of tumor formation with PDLIM4 overexpression suggest that PDLIM4 may function as tumor-suppressor gene in prostate cancer.

Mobilization of the actin cytoskeleton is an important process to generate a remarkable diversity of morphological behaviors, including motility and phagocytosis (33). Actin reorganization participates in aspects of cell proliferation including gene transcription and cytokinesis. It has been shown that a group of PDZ-LIM proteins, which comprises Cypher/ZASP, ENH, CLP36, mystique, ALP, and PDLIM4, associates with the actin cytoskeleton through interaction with α-actinin (34). PDLIM4 overexpression in osteosarcoma U20S cells was reported to change the dynamics of actin in stress fibers, with high formation and collapse of new fibers (35). The underlying molecular mechanism by which PDLIM4 suppresses prostate cancer cell proliferation is currently unknown. In our study, we provided the experimental evidence of the direct binding of PDLIM4 to F-actin. It has been suggested that F-actin may play a critical role in regulation of cell growth as well as many important signaling pathways (36, 37). Previous reports have shown that cells transformed by oncogenes usually exhibit some common features of disorganized actin filaments and focal adhesions which could in fact induce both anchorage-independent growth and cellular tumorigenicity (38, 39). Our data suggest that PDLIM4 localization to the actin-cytoskeleton may potentially play a role in suppression of cancer cell-proliferation and growth-inhibitory function.

In summary, the transcriptional silencing and loss of expression of PDLIM4 in prostate cancer cells, suppression of cellular proliferation, clonogenic and tumor growth indicate that

PDLIM4 might be involved in regulation of proliferation by associating with actin that could regulate the cytoskeletal function. This data seems to suggest that PDLIM4 may have additional properties that can affect tumor growth in xenograft. Further studies are required to address the role of this gene in the development and progression of the cancer.

Acknowledgments

This work was supported in part by NIH grants R01 AR049277 and CA70892.

References

1. Figueroa JA, De Raad S, Speights VO, Rinehart JJ. Gene expression of insulin-like growth factors and receptors in neoplastic prostate tissues: correlation with clinico-pathological parameters. Cancer Invest. 2001; 19(1):28–34. [PubMed: 11291553]
2. Dhanasekaran SM, Barrette TR, Ghosh D, Shah R, Varambally S, Kurachi K, Pienta KJ, Rubin MA, Chinnaiyan AM. Delineation of prognostic biomarkers in prostate cancer. Nature. 2001; 412(6849): 822–826. [PubMed: 11518967]
3. LaTulippe E, Satagopan J, Smith A, Scher H, Scardino P, Reuter V, Gerald WL. Comprehensive gene expression analysis of prostate cancer reveals distinct transcriptional programs associated with metastatic disease. Cancer Res. 2002; 62(15):4499–4506. [PubMed: 12154061]
4. Vanaja DK, Cheville JC, Iturria SJ, Young CY. Transcriptional silencing of zinc finger protein 185 identified by expression profiling is associated with prostate cancer progression. Cancer Res. 2003; 63(14):3877–3882. [PubMed: 12873976]
5. Vanaja DK, Ballman KV, Morlan BW, Cheville JC, Neumann RM, Lieber MM, Tindall DJ, Young CY. PDLIM4 repression by hypermethylation as a potential biomarker for prostate cancer. Clin Cancer Res. 2006; 12(4):1128–1136. [PubMed: 16489065]
6. Welsh JB, Sapinoso LM, Su AI, Kern SG, Wang-Rodriguez J, Moskaluk CA, Frierson HF Jr, Hampton GM. Analysis of gene expression identifies candidate markers and pharmacological targets in prostate cancer. Cancer Res. 2001; 61(16):5974–5978. [PubMed: 11507037]
7. Varambally S, Yu J, Laxman B, Rhodes DR, Mehra R, Tomlins SA, Shah RB, Chandran U, Monzon FA, Becich MJ, Wei JT, Pienta KJ, Ghosh D, Rubin MA, Chinnaiyan AM. Integrative genomic and proteomic analysis of prostate cancer reveals signatures of metastatic progression. Cancer Cell. 2005; 8(5):393–406. [PubMed: 16286247]
8. Yu YP, Landsittel D, Jing L, Nelson J, Ren B, Liu L, Mc-Donald C, Thomas R, Dhir R, Finkelstein S, Michalopoulos G, Becich M, Luo JH. Gene expression alterations in prostate cancer predicting tumor aggression and preceding development of malignancy. J Clin Oncol. 2004; 22(14):2790–2799. [PubMed: 15254046]
9. Boumber YA, Kondo Y, Chen X, Shen L, Gharibyan V, Konishi K, Estey E, Kantarjian H, Garcia-Manero G, Issa JP. RIL, a LIM gene on 5q31, is silenced by methylation in cancer and sensitizes cancer cells to apoptosis. Cancer Res. 2007; 67(5):1997–2005. [PubMed: 17332327]
10. Baird K, Davis S, Antonescu CR, Harper UL, Walker RL, Chen Y, Glatfelter AA, Duray PH, Meltzer PS. Gene expression profiling of human sarcomas: insights into sarcoma biology. Cancer Res. 2005; 65(20):9226–9235. [PubMed: 16230383]
11. Henderson SR, Guiliano D, Presneau N, McLean S, Frow R, Vujovic S, Anderson J, Sebire N, Whelan J, Athanasou N, Flanagan AM, Boshoff C. A molecular map of mesenchymal tumors. Genome Biol. 2005; 6(9):R76. [PubMed: 16168083]
12. Webber MM, Bello D, Kleinman HK, Hoffman MP. Acinar differentiation by nonmalignant immortalized human prostatic epithelial cells and its loss by malignant cells. Carcinogenesis. 1997; 18(6):1225–1231. [PubMed: 9214606]
13. Hunter CS, Rhodes SJ. LIM-homeodomain genes in mammalian development and human disease. Mol Biol Rep. 2005; 32(2):67–77. [PubMed: 16022279]
14. te Velthuis AJ, Bagowski CP. PDZ and LIM domain-encoding genes: molecular interactions and their role in development. Scientific World Journal. 2007; 7:1470–1492. [PubMed: 17767364]

15. Xia H, Winokur ST, Kuo WL, Altherr MR, Bredt DS. Actinin-associated LIM protein: identification of a domain interaction between PDZ and spectrin-like repeat motifs. J Cell Biol. 1997; 139(2):507–515. [PubMed: 9334352]

16. Guy PM, Kenny DA, Gill GN. The PDZ domain of the LIM protein enigma binds to beta-tropomyosin. Mol Biol Cell. 1999; 10(6):1973–1984. [PubMed: 10359609]

17. Vallenius T, Luukko K, Makela TP. CLP-36 PDZ-LIM protein associates with nonmuscle alpha-actinin-1 and alpha-actinin-4. J Biol Chem. 2000; 275(15):11100–11105. [PubMed: 10753915]

18. Vallenius T, Makela TP. Clik1: a novel kinase targeted to actin stress fibers by the CLP-36 PDZ-LIM protein. J Cell Sci. 2002; 115(Pt 10):2067–2073. [PubMed: 11973348]

19. Kang S, Xu H, Duan X, Liu JJ, He Z, Yu F, Zhou S, Meng XQ, Cao M, Kennedy GC. PCD1, a novel gene containing PDZ and LIM domains, is overexpressed in several human cancers. Cancer Res. 2000; 60(18):5296–5302. [PubMed: 11016661]

20. Tobias ES, Hurlstone AF, MacKenzie E, McFarlane R, Black DM. The TES gene at 7q31.1 is methylated in tumours and encodes a novel growth-suppressing LIM domain protein. Oncogene. 2001; 20(22):2844–2853. [PubMed: 11420696]

21. Fujimoto N, Yeh S, Kang HY, Inui S, Chang HC, Mizokami A, Chang C. Cloning and characterization of androgen receptor coactivator, ARA55, in human prostate. J Biol Chem. 1999; 274(12):8316–8321. [PubMed: 10075738]

22. Muller JM, Isele U, Metzger E, Rempel A, Moser M, Pscherer A, Breyer T, Holubarsch C, Buettner R, Schule R. FHL2, a novel tissue-specific coactivator of the androgen receptor. Embo J. 2000; 19(3):359–369. [PubMed: 10654935]

23. Gao J, Arbman G, Rearden A, Sun XF. Stromal staining for PINCH is an independent prognostic indicator in colorectal cancer. Neoplasia. 2004; 6(6):796–801. [PubMed: 15720806]

24. Chene L, Giroud C, Desgrandchamps F, Boccon-Gibod L, Cussenot O, Berthon P, Latil A. Extensive analysis of the 7q31 region in human prostate tumors supports TES as the best candidate tumor suppressor gene. Int J Cancer. 2004; 111(5):798–804. [PubMed: 15252854]

25. Sharp TV, Munoz F, Bourboulia D, Presneau N, Darai E, Wang HW, Cannon M, Butcher DN, Nicholson AG, Klein G, Imreh S, Boshoff C. LIM domains-containing protein 1 (LIMD1), a tumor suppressor encoded at chromosome 3p21.3, binds pRB and represses E2F-driven transcription. Proc Natl Acad Sci USA. 2004; 101(47):16531–16536. [PubMed: 15542589]

26. Kim AC, Peters LL, Knoll JH, Van Huffel C, Ciciotte SL, Kleyn PW, Chishti AH. Limatin (LIMAB1), an actin-binding LIM protein, maps to mouse chromosome 19 and human chromosome 10q25, a region frequently deleted in human cancers. Genomics. 1997; 46(2):291–293. [PubMed: 9417918]

27. Song Y, Maul RS, Gerbin CS, Chang DD. Inhibition of anchorage-independent growth of transformed NIH3T3 cells by epithelial protein lost in neoplasm (EPLIN) requires localization of EPLIN to actin cytoskeleton. Mol Biol Cell. 2002; 13(4):1408–1416. [PubMed: 11950948]

28. van den Berk LC, van Ham MA, te Lindert MM, Walma T, Aelen J, Vuister GW, Hendriks WJ. The interaction of PTP-BL PDZ domains with RIL: an enigmatic role for the RIL LIM domain. Mol Biol Rep. 2004; 31(4):203–215. [PubMed: 15663004]

29. Cuppen E, van Ham M, Wansink DG, de Leeuw A, Wieringa B, Hendriks W. The zyxin-related protein TRIP6 interacts with PDZ motifs in the adaptor protein RIL and the protein tyrosine phosphatase PTP-BL. Eur J Cell Biol. 2000; 79(4):283–293. [PubMed: 10826496]

30. Sasso FC, Carbonara O, Persico E, D'Ambrosio R, Coppola L, Nasti R, Campana B, Moschella S, Torella R, Cozzolino D. Increased vascular endothelial growth factor mRNA expression in the heart of streptozotocin-induced diabetic rats. Metabolism. 2003; 52(6):675–678. [PubMed: 12800090]

31. Bashirova AA, Markelov ML, Shlykova TV, Levshenkova EV, Alibaeva RA, Frolova EI. The human RIL gene: mapping to human chromosome 5q31.1, genomic organization, and alternative transcripts. Gene. 1998; 210(2):239–245. [PubMed: 9573374]

32. Le Beau MM, Espinosa R 3rd, Neuman WL, Stock W, Roulston D, Larson RA, Keinanen M, Westbrook CA. Cytogenetic and molecular delineation of the smallest commonly deleted region of chromosome 5 in malignant myeloid diseases. Proc Natl Acad Sci USA. 1993; 90(12):5484–5488. [PubMed: 8516290]

33. Yeh BJ, Rutigliano RJ, Deb A, Bar-Sagi D, Lim WA. Rewiring cellular morphology pathways with synthetic guanine nucleotide exchange factors. Nature. 2007; 447(7144):596–600. [PubMed: 17515921]
34. Tamura N, Ohno K, Katayama T, Kanayama N, Sato K. The PDZ-LIM protein CLP36 is required for actin stress fiber formation and focal adhesion assembly in BeWo cells. Biochem Biophys Res Commun. 2007; 364(3):589–594. [PubMed: 17964547]
35. Vallenius T, Scharm B, Vesikansa A, Luukko K, Schafer R, Makela TP. The PDZ-LIM protein RIL modulates actin stress fiber turnover and enhances the association of alpha-actinin with F-actin. Exp Cell Res. 2004; 293(1):117–128. [PubMed: 14729062]
36. Lamalice L, Le Boeuf F, Huot J. Endothelial cell migration during angiogenesis. Circ Res. 2007; 100(6):782–794. [PubMed: 17395884]
37. Meyers JR, Corwin JT. Shape change controls supporting cell proliferation in lesioned mammalian balance epithelium. J Neurosci. 2007; 27(16):4313–4325. [PubMed: 17442815]
38. Pollock CB, Shirasawa S, Sasazuki T, Kolch W, Dhillon AS. Oncogenic K-RAS is required to maintain changes in cytoskeletal organization, adhesion, and motility in colon cancer cells. Cancer Res. 2005; 65(4):1244–1250. [PubMed: 15735008]
39. Barros JC, Marshall CJ. Activation of either ERK1/2 or ERK5 MAP kinase pathways can lead to disruption of the actin cytoskeleton. J Cell Sci. 2005; 118(Pt 8):1663–1671. [PubMed: 15797923]

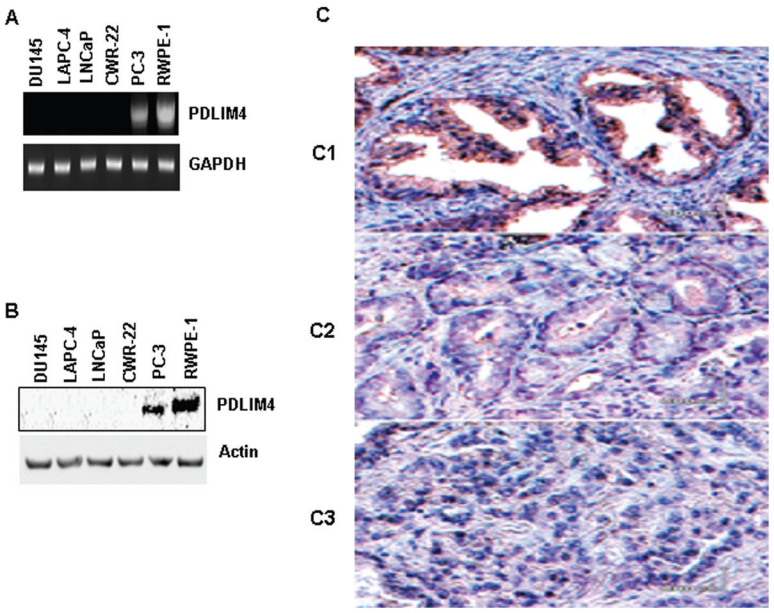

Figure 1.

Expression of PDLIM4 mRNA and protein in various human prostate cell lines. (A) PDLIM4 mRNA levels in human prostate cell lines by RT-PCR. GAPDH mRNA is used as housekeeping control. (B) PDLIM4 protein expression in human prostate cell lines by Western blot analysis with an anti-PDLIM4 antibody. Actin staining of blots after transfer revealed equivalent loading of total protein. (C) Detection of PDLIM4 protein expression in benign prostate and prostate cancer tissues by immunohistochemistry. C1 is representative PDLIM4 staining in benign prostate tissue showing reddish brown PDLIM4 staining of the secretory epithelial cells. C2 and C3 are prostate cancer Gleason grade-6 and Gleason grade-9 tissues with a reduced level of PDLIM4 staining. Preimmune serum or normal rabbit IgG was used as a control and showed no staining (data not shown).

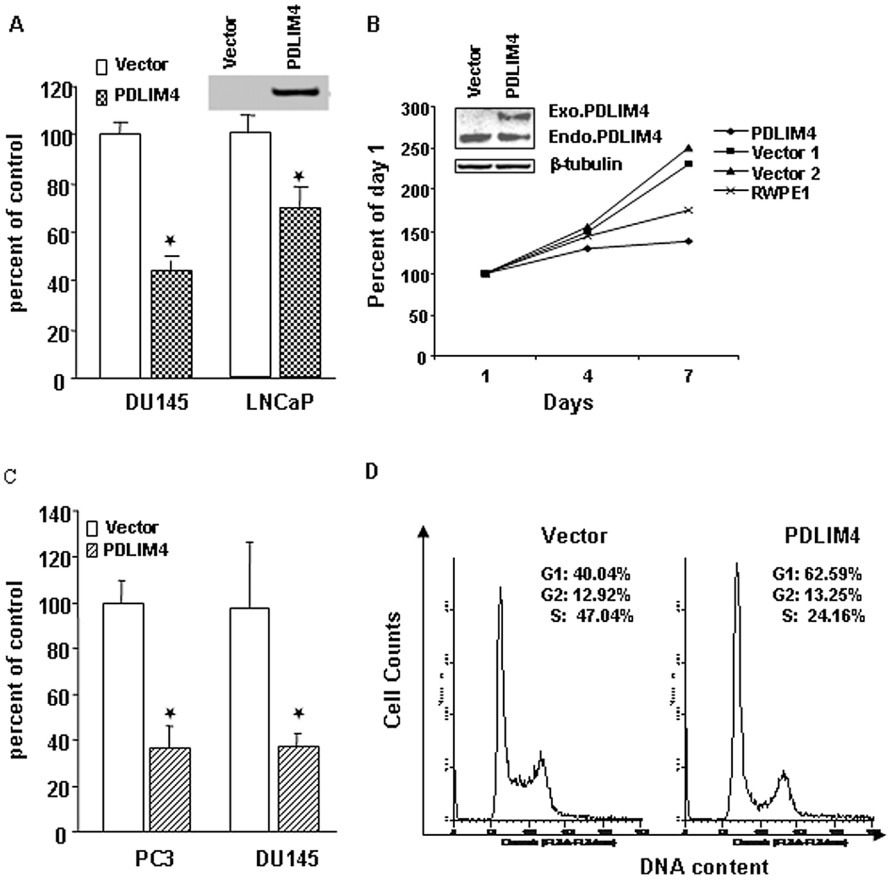

Figure 2.

Effects of PDLIM4 overexpression on prostate cancer cell growth. (A) Cell growth of PDLIM4 transient-transfected DU145 and LNCaP cells compared to vector control. Cell growth was determined on day 7 by MTS assay. The insert shows expression of PDLIM4 detected by V5 antibody. Bars, SD, *, $p < 0.05$, versus vector control group. (B) Cell growth of PDLIM4 stable-transfected PC3 cells (PDLIM4 clone) compared to the empty vector V-5 clones 1 and 2 (vector #1 and 2). MTS assay was performed on day 1, 4, and 7 as indicated. Insert shows PDLIM4 protein-expression levels in stable transfected PC3 cells (exogenous and endogenous PDLIM4) and vector control clone (endogenous PDLIM4 only) by western blotting. (C) Anchorage independent growth of cells by PDLIM4 overexpression. PC-3 and DU145 cells after transfection with PDLIM4 or empty vector were grown in soft agar media. The average colony number for the vector control was set at 100% and the cell growth of PDLIM4-transfected cells is shown as percentage of the control. Bars, SD, *, $p < 0.001$, versus vector control group. (D) Cell-cycle distribution of PC3 cells determined by a FACScan flow cytometer by transfection with PDLIM4 or vector control. Percentage of cells in G1, G2, and S phase are shown.

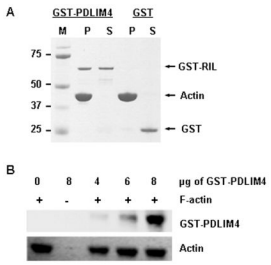

Figure 3.

Association of PDLIM4 with F-actin. Cosedimentation assay was performed using GST-PDLIM4 and F-actin. The GST-PDLIM4, GST, and F-actin in supernatants and pellets were determined by NuPAGE gel. (A) Coomassie-blue-staining of the gel (M: marker, P: pellet, S: supernatant). (B) Western blot analysis. Antibody against GST was used to determine which sediments contained GST-PDLIM4. Actin shown in the lowest row represents the amount of actin in each fraction.

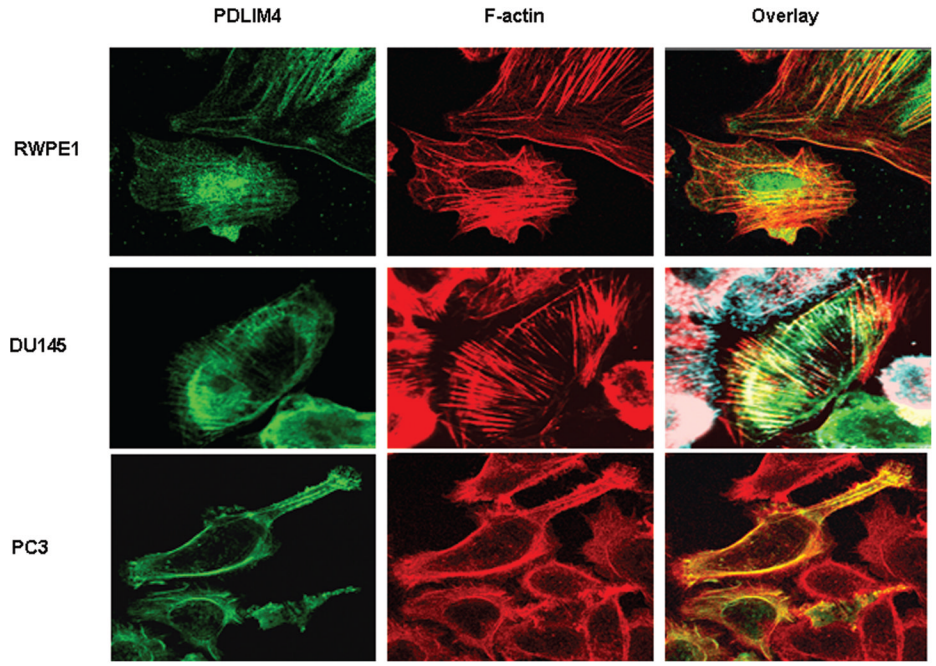

Figure 4.

Colocalization of PDLIM4 with F-actin in prostate cell lines. Expression of endogenous PDLIM4 in RWPE-1, DU145, and PC3 cells. Fluorescent images were captured in a Zeiss LSM 510 laser-scanning confocal microscope. Endogenous PDLIM4 and the colocalization with F-actin are shown in RWPE1 cells. DU145 and PC3 cells were transfected with PDLIM4-V5 expression vector overnight, fixed, permeabilized, and stained with antibodies. Cells were stained with anti-PDLIM4 antibody and FITC-labeled secondary antibody (green) for PDLIM4. Rhodamine phalloidin (red) staining was used for F-actin. Yellow-orange color in overlay shows various degrees of colocalization of PDLIM4 and F-actin.

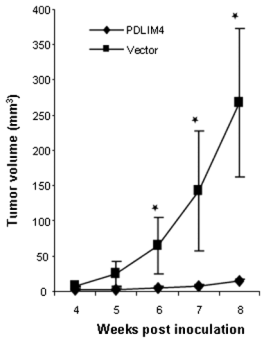

Figure 5.

In vivo effect of PDLIM4 expression in prostate cancer cells on tumor growth. BALB/c (nu/nu) mice (n = 4 each group) were inoculated with PDLIM4 stable cells and vector control stable cells subcutaneously. From the time of palpable tumors (4 weeks), tumor size was measured every week up to 8 weeks and tumor volume was calculated. Bars, SD, *, $p < 0.05$, versus vector control group.